

Original Article

Open Access



[¹⁸F]FDG PET imaging evaluation on non-alcoholic fatty liver disease and hepatocellular carcinoma model treated with sorafenib

Fernando Gomes de Barros Costa¹, José Tadeu Stefano¹, Daniele de Paula Faria², Caio de Souza Levy¹, Maria Cristina Chammas³, Camila de Godoi Carneiro², Isabel Veloso Alves Pereira⁴, Bruno Cogliati⁴, Flair José Carrilho¹, Claudia P. Oliveira¹

¹Department of Gastroenterology (LIM-07), University of São Paulo School of Medicine, São Paulo 01246-903, Brazil.

²Nuclear Medicine Laboratory (LIM-43), Radiology and Oncology Department, University of São Paulo School of Medicine, São Paulo 01246-903, Brazil.

³Radiology and Oncology Department, University of São Paulo School of Medicine, São Paulo, São Paulo 01246-903, Brazil.

⁴Department of Pathology, School of Veterinary Medicine and Animal Science, University of São Paulo, São Paulo 05808-010, Brazil.

Correspondence to: Dr. Fernando Gomes de Barros Costa, Department of Gastroenterology (LIM-07), University of São Paulo School of Medicine, Lim-07 Ave. Dr. Arnaldo, São Paulo 01246-903, Brazil. E-mail: fgbcosta85@gmail.com; Dr. Claudia P. Oliveira, Department of Gastroenterology (LIM-07), University of São Paulo School of Medicine, Lim-07 Ave. Dr. Arnaldo, São Paulo 01246-903, Brazil. E-mail: claudia.oliveira220@fm.usp.br

How to cite this article: Costa FGB, Stefano JT, Faria DP, Levy CS, Chammas MC, Carneiro CG, Pereira IVA, Cogliati B, Carrilho FJ, Oliveira CP. [¹⁸F]FDG PET imaging evaluation on non-alcoholic fatty liver disease and hepatocellular carcinoma model treated with sorafenib. *Hepatoma Res* 2018;4:35. <http://dx.doi.org/10.20517/2394-5079.2018.06>

Received: 8 Feb 2018 **First Decision:** 9 Mar 2018 **Revised:** 11 May 2018 **Accepted:** 11 May 2018 **Published:** 12 Jul 2018

Science Editor: Guang-Wen Cao **Copy Editor:** Jun-Yao Li **Production Editor:** Cai-Hong Wang

Abstract

Aim: Evaluate the effect of sorafenib in a rat model of non-alcoholic fatty liver disease (NAFLD) related to hepatocellular carcinoma (HCC) by quantifying the correlation between changes in glucose metabolism on PET imaging and degree of tumor differentiation.

Methods: NAFLD related HCC was induced by the combination of high fat and choline deficient diet with diethylnitrosamine (100 mg/L) for 16 weeks. Then carcinogenic stimuli were suspended, liver nodules were identified by abdominal ultrasound and two groups were randomized: control ($n = 10$) and sorafenib ($n = 20$). Rats received daily gavage administration of 1 mL saline or sorafenib (5 mg/kg/day) for more 3 weeks. After treatment, [¹⁸F]FDG PET scan was performed on animals.

Results: [¹⁸F]FDG uptake was lower in the sorafenib group than that in the control group (3.3 ± 0.48 vs. 5.5 ± 1.5 , $P = 0.01$). Direct correlation was found between poorly-differentiated HCC and TumorSUVmax/MuscleSUVmax ratio ($R^2 = 0.54$, $P = 0.006$). Treatment was associated with significantly more residual tumors that were well differentiated (Grades I/II) than in the untreated control group (39% vs. 5%, respectively, $P = 0.01$).



© The Author(s) 2018. **Open Access** This article is licensed under a Creative Commons Attribution 4.0 International License (<https://creativecommons.org/licenses/by/4.0/>), which permits unrestricted use, sharing, adaptation, distribution and reproduction in any medium or format, for any purpose, even commercially, as long as you give appropriate credit to the original author(s) and the source, provide a link to the Creative Commons license, and indicate if changes were made.



Conclusion: Sorafenib shows promise as a treatment for reducing the aggressiveness of HCC as demonstrated by [¹⁸F] FDG PET and immunohistochemistry.

Keywords: Animal model, hepatocellular carcinoma, liver steatosis, non-alcoholic fatty liver disease, positron emission tomography, sorafenib

INTRODUCTION

Non-alcoholic, fatty liver disease (NAFLD) is associated with obesity and known to progress to non-alcoholic, steatohepatitis (NASH), cirrhosis and then hepatocellular carcinoma (HCC), or directly progress from NASH to HCC^[1-3]. Liver cancer is the 16th cause of global mortality and HCC accounts for up to 90% of all primary liver cancers^[4,5]. Observational studies showed that diabetes, obesity, and iron overload are risk factors for development of HCC and NAFLD^[2].

Animal models are crucial to elucidate the physiopathology of HCC and to test potential therapeutic targets^[6,7]. The ideal model of NAFLD-related HCC should replicate human HCC development, given a high caloric diet, obesity, insulin resistance, dyslipidemia, similar hepatic markers, natural evolution of HCC, genetic aspects and activation of the same signaling pathways^[8,9]. There are many animal models for HCC that include genetically altered animals and orthotopic tumor implantation, however they are not ideal to replicate NAFLD as they do not exhibit liver and metabolic changes^[7,10]. Previous work used a mixed experimental model of NAFLD-related HCC with fat and choline deficient diets together with diethylnitrosamine (DEN) in drinking water to achieve HCC development within 16 weeks; a shorter period than usual^[7,11]. DEN has been used as a carcinogen and is capable of inducing HCC with intra- and inter-tumor variability as it occurs in humans^[12-14].

Earlier studies performed with HCC patients, treated with sorafenib, demonstrated that higher values of 2-deoxy-2-[¹⁸F]-fluoro-D-glucose ([¹⁸F]FDG) uptake (expressed as SUVmax) were correlated with lower overall survival and more advanced HCC^[15-21]. In HCC cell lines, the absence of p53 expression is indicative of a worse prognosis, as is the increased [¹⁸F]FDG uptake^[22]. A recent metabolic study of HCC by positron emission tomography ([¹⁸F]FDG PET) showed that this imaging technique could be a prognostic tool, as results correlate with long-term survival and early recurrence of HCC after liver transplantation^[21,23]. This tool can be used to identify the most undifferentiated and aggressive tumors to select patients who should undergo liver transplantation^[17].

Sorafenib was the first drug approved by the FDA for treatment of advanced HCC (BCLC C)^[24,25]. The usual dose for humans is 800 mg/day, providing an average of 127 μmol/L/h of plasmatic concentration (AUC_{0-12h}), while the equivalent dosage in rats is 5 mg/kg/day^[26-28]. It had been showed that sorafenib (2.5 mg/kg/day) has the capacity to prevent hepatic fibrosis, mitochondrial dysfunction, and reduce inflammation (interleukines 6 and 10) in NAFLD animal models^[29]. Furthermore, Yang *et al.*^[30] tested it for 8 weeks (5 mg/kg/day) and demonstrated that sorafenib improved hepatic venous dysregulation, inhibited recruitment and activation of leukocytes, and reduced splanchnic vasodilatation and ascites.

This study aimed to evaluate the effect of sorafenib in a rat model of NAFLD related to HCC by using [¹⁸F] FDG PET imaging as a tool to quantitate the degree of HCC differentiation *in vivo*.

METHODS

This study was approved by the ethical committee for animal use of the University of Sao Paulo Medical School (protocol 108/14), following the current standards of small animal care.

Thirty male Sprague-Dawley rats weighing 300-400 g at 8 weeks of age were used. HCC secondary to NAFLD was induced by high fat and choline deficient diets [35% of total fat, enriched with 54% of trans-fatty acids (Rhoster Ltd., BR)], with a DEN (Sigma-Aldrich Chemical, St. Louis, MO, USA) dose of 100 mg/L in the drinking water ad libitum for 16 weeks. After this period stimuli were suspended and the animals were randomly split into 2 groups. The control group ($n = 10$) received 1 mL of saline solution (0.9%) daily by gavage for 3 more weeks. The sorafenib group ($n = 20$) received 5 mg/kg/day of sorafenib (Bayer Healthcare Pharmaceuticals, Cologne, GY) by gavage for 3 more weeks.

At 16 weeks, rats were anesthetized with ketamine 80 mg/kg (Cristalia, BR) and xylazine 10 mg/kg (Bayer, BR) intraperitoneally and then submitted to abdominal ultrasound (US) to quantify, measure, and localize hepatic nodules^[31]. Board-certificated radiologist (M.C.C) with 24 years of experience performed the procedure using a Philips Ultrasound IU 22 system (Bothell, WA, USA) with a VL13-5 transducer. Only nodules larger than 0.2 cm were considered and catalogued in the distribution of parenchyma: left lobe, right lobe, medium lobe, and caudate lobe.

PET images with [¹⁸F]FDG were acquired at the end of treatment (3 weeks after initial sorafenib) in a small animal PET scanner (LabPET4 Gamma Medica-Ideas, Northridge, CA, USA), using methods similar to those outlined in Park *et al.*^[15]. Animals were anesthetized with isoflurane 5% in oxygen 100% for induction and 2%-3% for maintenance. [¹⁸F]FDG was injected in the penile vein (37.7 ± 6.29 MBq) and the animals were allowed to wake up after injection for better tracer distribution. After 45 min of tracer injection the animals were anesthetized again and the image acquired for 30 min. Computed tomography (CT) images were also obtained with 65 kVp, 165 μ A in 512 projections and magnification of 1.3 for anatomic correlation.

PET images were reconstructed by the ordered subsets expectation-maximization 3D (OSEM-3D) method^[32] with 20 interactions, 4 subsets, a transverse field of view of 100 mm, and a matrix of 240×240 , for pixel resolution of $0.42 \text{ mm} \times 0.42 \text{ mm}$. The CT images were reconstructed with a filtered back projection method, a matrix of 512×512 , and pixel resolution of $0.17 \text{ mm} \times 0.17 \text{ mm}$. CT images were used for attenuation correction of the PET images.

Images were analyzed by the PMOD™ software (PMOD Technologies Ltd., Zurich, CH) to obtain quantitative measures of [¹⁸F]FDG uptake in defined regions of interest in the rats in each group. The visualization interface in the software allowed regions of interest (ROI) to be drawn specifically and entirely within tumor lesions, liver tissue and muscle. The uptake values were expressed as using the dose-normalized parameter standardized uptake value (SUV). $\text{SUV} = \text{radioactivity concentration (kBq/mL)} / [\text{injected dose (kBq)} / \text{animal weight (g)}]$. The maximum value of the SUV within a region of interest is expressed as SUVmax.

Three days after the PET scan (week 19), the rats were euthanized with dextroketaamine (Cristalia, BR) 120 mg/kg and xylazine (Bayer, BR) 10 mg/kg intraperitoneally. Liver samples of the right and left lobes and the larger tumors evidenced in PET/CT were collected for histological analysis. The liver specimens were fixed in 4% formaldehyde and stained with hematoxylin-eosin (HE). These samples were blindly scored by a veterinary hepatopathologist (B.C) with 12 years of experience, using a modified classification standardized by Kleiner *et al.*^[33]. The variables analyzed were steatosis (0-3), lobular inflammatory changes (0-3), hepatocyte ballooning (0-2), fibrosis (0-4), and ductular reaction (0-3) through the NALFD activity score (NAS)^[33]. HCC was diagnosed with characteristics defined by Thoolen *et al.*^[34] for rats and then classified by Schlageter *et al.*^[35]. Histological classifications are considered the gold standard for assessment of HCC and are used in this study to evaluate the performance of the non-invasive characterization using ¹⁸F-FDG PET.

Immunohistochemical analysis was performed for protein glutamine synthetase (GS), hepatocyte specific antigen (HEP-PAR-1), and cytokeratin 19 (CK-19). HCC was considered for nodules with positive results for

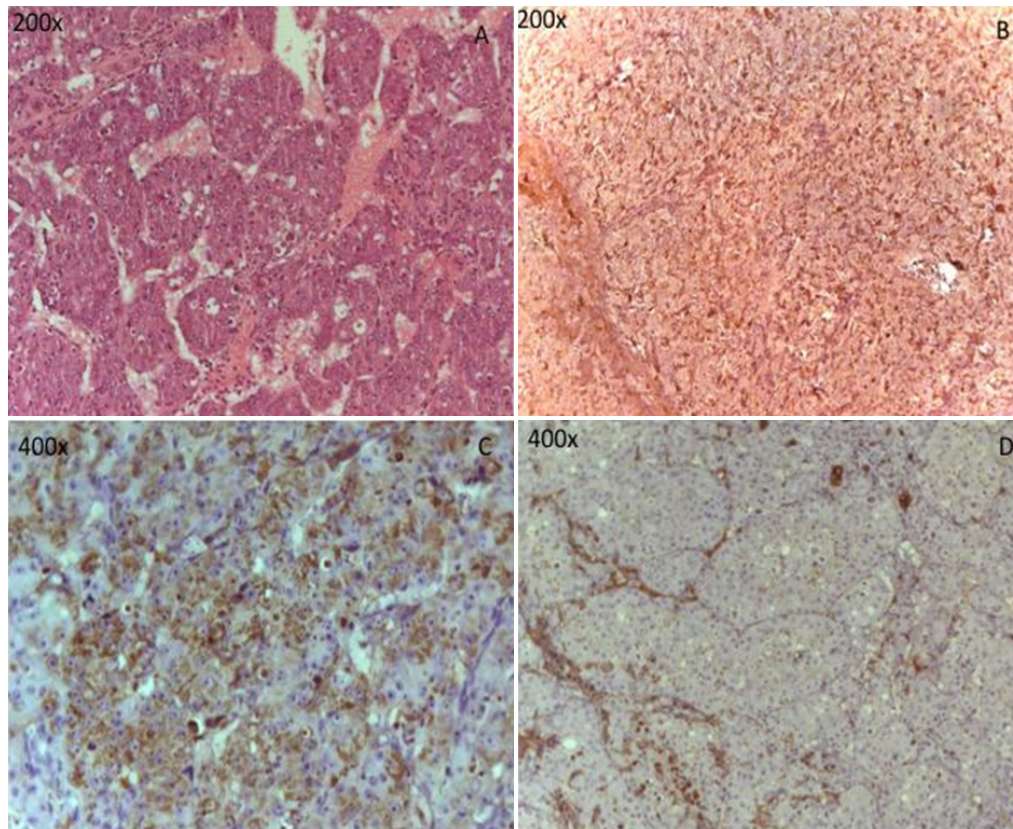


Figure 1. Illustrations of histologic and immunohistochemical view of the HCC Grade III Edmondson-Steiner. (A) Hematoxylin-eosin, $\times 200$; (B) glutamine synthetase, $\times 200$; (C) HEP-PAR-1, $\times 400$; (D) CK-19, $\times 400$

GS or HEP-PAR-1, and negative for CK-19 [Figure 1]. Antibody dilution was GS 1:3000, HEP-PAR-1 1:500 and CK-19 1:200. The method used involved immunoperoxidase with antigenic recovery by humid heat.

Statistical analysis was done with Excel® and GraphPad Prism® 7.0. The Student *t*-test was used for Gaussian distribution variables and the Mann-Whitney test was used for non-Gaussian distribution variables. Calculation of descriptive statistics: mean, median, and standard deviation, was performed using the appropriate form of the statistic for the distribution pattern of variables. To compare histological findings with PET findings, chi-square, linear regression, Kruskal-Wallis and Tukey *post-hoc* tests were used. Only *P* values less than 0.05 were considered statistically relevant.

RESULTS

All animals completed the first 16 weeks, but between the 16th and 19th week, when the treatment began, animals' mortality reached 60% in both groups. The main causes of death were pneumonia, hemorrhagic ascites due to tumor rupture, included during anesthesia induction for PET scan. Mean survival in the sorafenib group was 130 ± 4.9 days with a median of 133 days, and the control group was 126.3 ± 8.5 days with a median of 130 days ($P = 0.07$). The animals' body weight did not show a statistical difference between groups during the study, however it was different at time of euthanasia [Table 1].

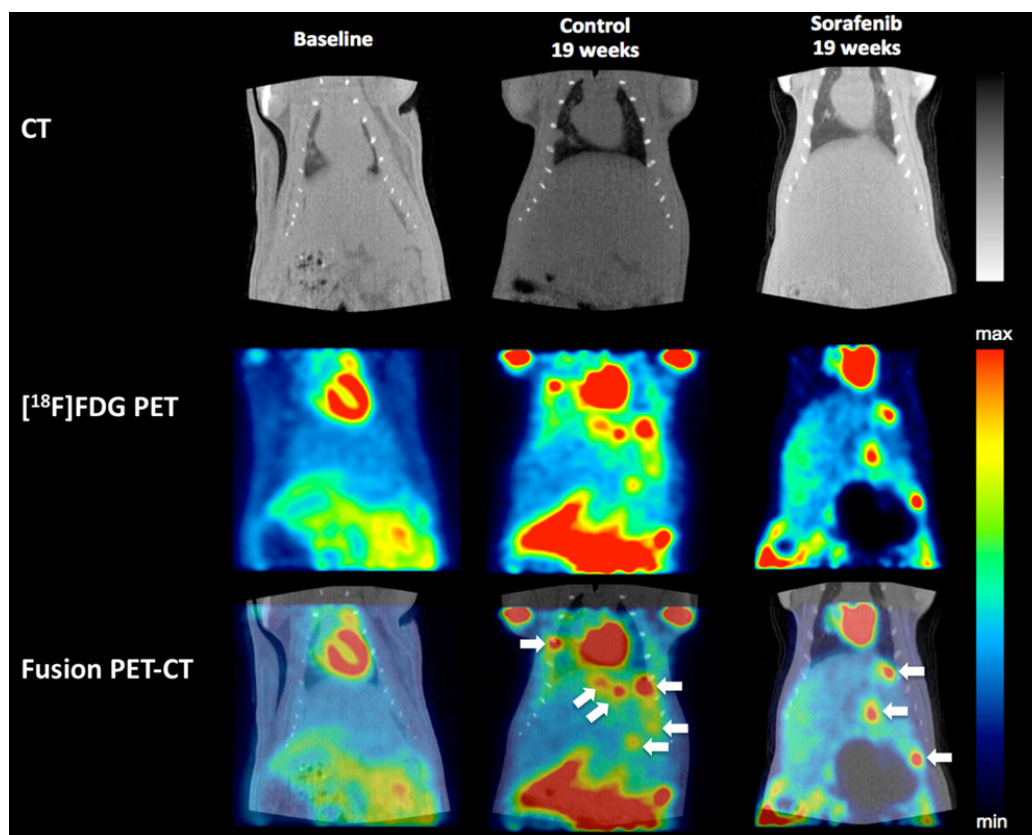
US findings showed no difference between groups regarding the average liver nodules distribution per animal (4.88 ± 2.75 in the control group vs. 4.95 ± 3.11 in the sorafenib group, $P = 0.48$) or major nodule size [Table 2]. The average number of nodules per animal detected by PET was 4.37 ± 1.59 in the sorafenib group and 8.5 ± 3.7 in the control group ($P = 0.006$) [Figure 2].

Table 1. Weight evolution according to studied groups

Weight (g)	Control average (n = 10)	Sorafenib average (n = 20)	P value
16th week	479.5 ± 45.4	463 ± 46.2	0.28
19th week	440.5 ± 67	420 ± 34.4	0.24
Euthanasia	486.3 ± 38	394 ± 48.5	0.003
Liver weight	35 ± 4.6	27.5 ± 11.6	0.13

Table 2. The sonographic findings at the 16th week of experimentation before treatment with sorafenib or placebo

Liver US 16th week	Control (n = 10)	Sorafenib (n = 20)	P value
Major nodule (cm)	1.04 ± 0.69	0.72 ± 0.92	0.34
Median of nodules per animal	5	5	
Average of nodules per animal	4.88 ± 2.75	4.95 ± 3.11	0.48
Quantity of nodules	44	99	
Percent of nodules in the left/medium lobes	75	61	0.14
Percent of nodules in the right/caudate lobes	25	39	0.22
Percent of ascites	11	10	0.46

**Figure 2.** Illustrative images of the CT, PET with [¹⁸F]FDG, and fusion PET/CT. Note that the sorafenib group shows 3 high uptake lesions in the liver, while the control group shows 5 high uptake lesions in the liver and 1 lesion in the right lung (indicated by white arrows in the fusion image)

[¹⁸F]FDG uptake (expressed in SUVmax) was different between the two groups: 2.4 ± 1.98 in the sorafenib group and 3.8 ± 1.74 in the control group ($P = 0.01$) [Figure 3]. According to HCC Edmondson-Steiner classification, SUVmax had this distribution: grade II, median 2.1 (1.72-4.93); grade III, median 3.86 (1.63-11.3); grade IV, median 4.87 (4.34-5.91); $P = 0.008$ [Figure 4]. Significant differences were seen between grade II vs. III ($P = 0.023$) and grade II vs. IV ($P = 0.013$), but between grade III and IV the differences were not significant ($P = 0.449$).

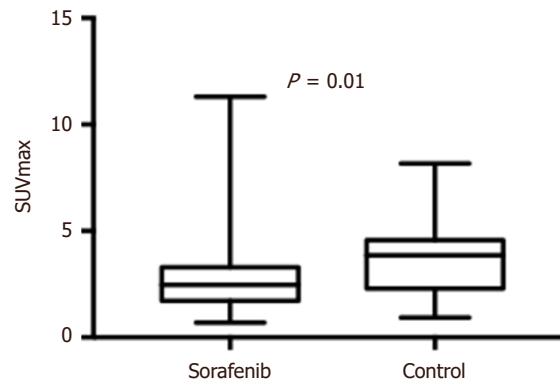


Figure 3. Comparison of SUVmax values between nodules of the control and sorafenib groups

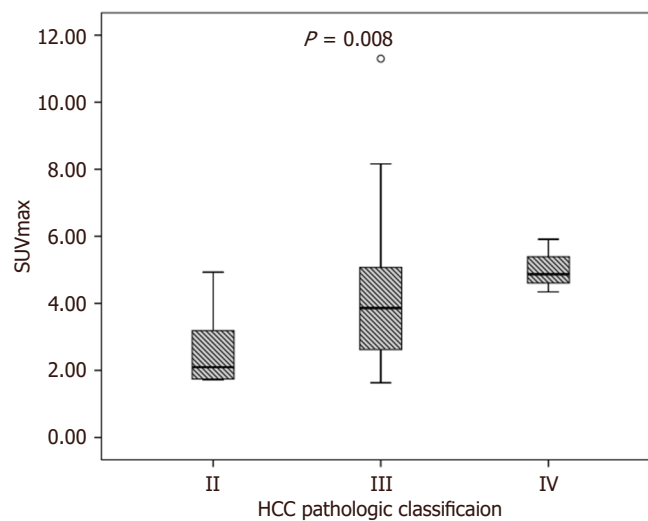


Figure 4. Comparison between SUVmax and HCC pathological classification

Correlation between less differentiated/undifferentiated HCC (Grades III/IV) and the highest values of [^{18}F] FDG uptake, presented as tumor SUVmax ($R^2 = 0.44$, $P = 0.01$) or as a tumor ratio, either Tumor SUVmax/Liver SUVmax ratio ($R^2 = 0.42$, $P = 0.02$) or Tumor SUVmax/SUVmax muscle ratio ($R^2 = 0.54$, $P = 0.006$) was found [Figure 5].

The pathology results showed that the sorafenib-treated group had more well-differentiated HCC (39% vs. 5%, respectively I/II vs. III/IV, $P = 0.01$), and less poorly-differentiated HCC (52% vs. 81%, respectively I/II vs. III/IV, $P = 0.003$). There was no difference between the two groups for necroinflammatory activity, degree of hepatic fibrosis, vascular invasion, intra-nodule hemorrhage, nodule necrosis, and low-grade dysplastic nodules [Table 3].

DISCUSSION

Our study is the first to evaluate the effect of sorafenib in a mixed experimental model of advanced HCC secondary to NAFLD using PET imaging with [^{18}F]FDG for quantitation of tumor growth. The decreased HCC nodules per animal in the treated group suggests the positive effect of sorafenib treatment, which is affirmed by the higher proportion of well-differentiated lesions (Edmondson-Steiner Grades I/II) in the treated group. The PET findings showing fewer lesions with high uptake per animal in the sorafenib group

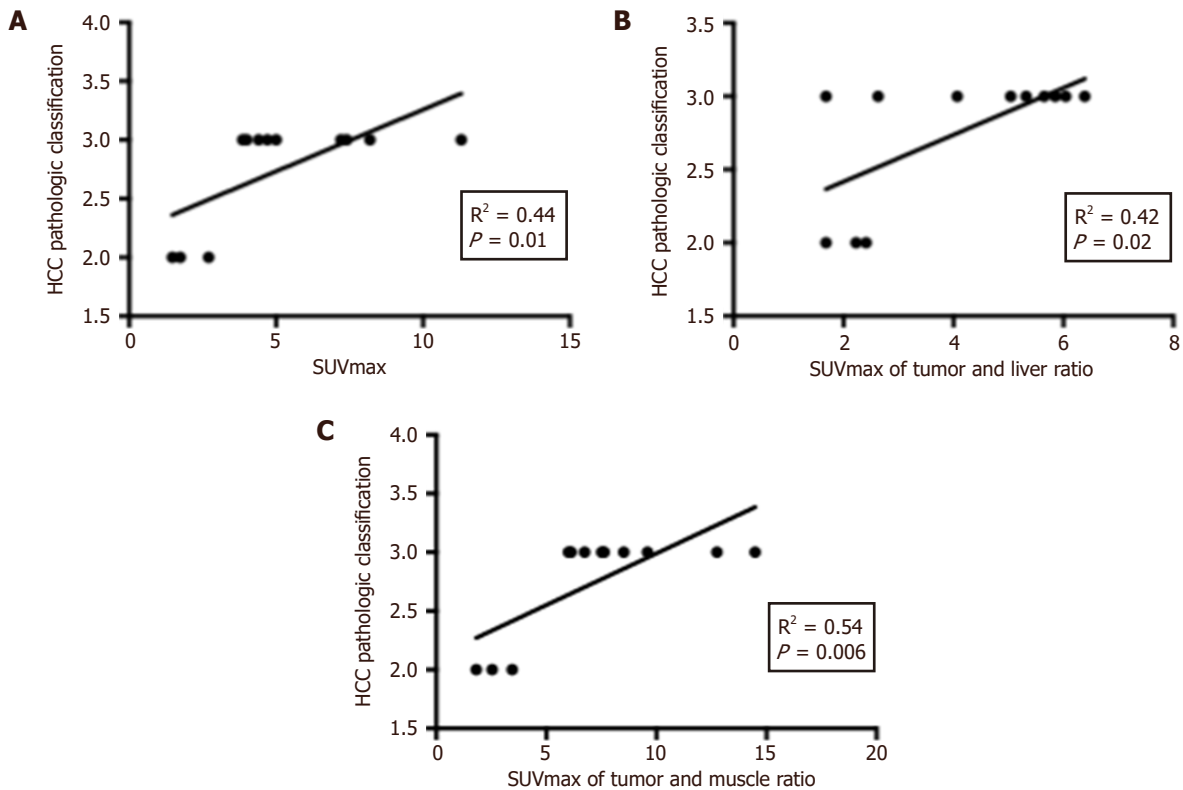


Figure 5. Dispersion graphs. (A) Plot of HCC Grade of differentiation and SUVmax taken by lesions; (B) plot of HCC Grade of differentiation and relation between tumor and liver tissue SUVmax; (C) plot of HCC Grade of differentiation and relation of tumor and muscle SUVmax. Correlation and P values are noted on the graphs

Table 3. Histological findings at the end of the study, showing differences and similarities between treated and control groups

Histological finding	Control	Sorafenib	P value
NAS 4	100% (4/4)	75% (6/8)	0.23
NAS 6	0% (0/4)	25% (2/8)	
Liver fibrosis stage 3	0% (0/4)	25% (2/8)	0.23
Liver fibrosis stage 4	100% (4/4)	75% (6/8)	
Vascular invasion	75%	43%	0.30
Intranodular hemorrhage	31% (7/22)	43% (10/23)	0.49
Intranodular necrosis	41% (9/22)	47% (11/23)	0.51
Low grade dysplastic lesions	14% (3/22)	9% (2/23)	0.24
Grade I/II HCC lesions	5% (1/22)	39% (9/23)	0.01
Grade III/IV HCC lesions	81% (18/22)	52% (12/23)	0.003

than in the control group ($P = 0.006$) also suggest the positive effect of sorafenib for decreasing undifferentiated lesions (Grades III/IV of Edmondson-Steiner).

Mattina et al.^[36] published a meta-analysis summarizing the antitumor efficacy of sorafenib in preclinical studies. They found that 95% of the models used human xenotransplants to assess effectiveness of the drug. Although most cell lines show robust action of sorafenib in mice, others like McA-RH7777 did not respond^[12]. In our study, we observed a decrease in the mean number of HCC lesions per animal, and a decrease in lesion aggressiveness; without a complete cure.

Groß et al.^[12] compared differences in the response of sorafenib between the model with isolated use of DEN in water for 8 weeks and a model inoculated with cancerous cells in the liver by injecting them in the portal vein. The DEN model had intra- and inter-tumoral variability, as it does in humans, while the cancer cells

were more homogeneous. In addition, sorafenib only acted on the DEN model, decreasing tumor growth and perfusion^[12]. Similar findings were demonstrated in another study that observed a low objective response (3%) by RECIST criteria^[37]. This cytotoxic response pattern was also observed in another clinical study, in which approximately 42% of patients were stable or had a minor/partial response^[38].

In the current study, we found the presence of advanced fibrosis or cirrhosis in all animals, as well as advanced HCC with vascular invasion in 75% of control animals ($n = 4$) and 43% of animals in the treated group ($n = 8$). These findings highlight the clinical relevance of our model, as most preclinical studies used younger animals with less advanced disease, thus not reflecting the hepatic microenvironment observed in humans^[36].

Despite treatment with sorafenib, the mortality rate (60%) was similar in both groups, resulting from the severity of liver cirrhosis and advanced HCC; sometimes with decompensation in ascites (about 10% in both groups) and pulmonary metastasis. In humans, the prognosis of advanced HCC is bleak, with a median survival of 6 months or 25% in 1 year^[24]. Park *et al.*^[15] used PET/CT with [¹⁸F]FDG to evaluate rats exposed only to intraperitoneal DEN, administered once a week for 16 weeks. They reported a mortality rate similar to our study, or about 65% in week 19. A more precise evaluation of the effect of sorafenib on survival was not possible because all animals were euthanized 3 days after the last PET scan to minimize risk of losing more animals prior to the endpoint of the study.

The development of a biochemical marker or diagnostic tool to identify the most undifferentiated and aggressive tumors has been studied in an attempt to better select patients for curative treatment^[17,24]. [¹⁸F]FDG PET appears to be a potential tool, because it has been shown that higher values of [¹⁸F]FDG uptake correlates with lower overall survival, advanced HCC, undifferentiated histology (loss of p53 expression), and increased liver transplantation recurrence^[17,19,22,39]. Lee *et al.*^[23] retrospectively evaluated patients who underwent liver transplantation for HCC and had [¹⁸F]FDG PET prior to surgery. They found that HCC patients with lower [¹⁸F]FDG uptake had more highly differentiated HCC (Grades I/II Edmondson-Steiner classification), with lower rates of microvascular invasion and no recurrence of HCC after a 3-year follow-up^[23]: results that are similar to the results found in our work.

Kim *et al.*^[17] showed that the [¹⁸F]FDG uptake calculated as ratio between tumor and liver adjacent tissue was more accurate than tumor uptake in predicting HCC post-transplant recurrence (SUVmax Tumor/SUVmax Liver 0.869 *vs.* tumor SUVmax 0.762). In our study, the best correlation of [¹⁸F]FDG uptake and HCC Grades at III/IV was found with SUVmax Tumor/SUVmax Muscle ($R^2 = 0.54$, $P = 0.006$), followed by SUVmax tumor ($R^2 = 0.44$, $P = 0.01$) and Tumor SUVmax/Liver SUVmax ratio ($R^2 = 0.42$, $P = 0.02$): somewhat lower than what was reported by Kim *et al.*^[17].

The absence of a pretreatment (16th week) [¹⁸F]FDG PET scan is one limitation of our study, as we could not follow the evolution of the same node with one diagnostic tool throughout the experiment. This decision was based on two reasons: (1) high probability of increasing mortality rate on additional anesthesia during image acquisition (animals were already weak at that point) and (2) at pretreatment time point it was necessary to ensure the presence of lesions that could be detected by PET (> 1 mm) at a later point in time; therefore, a method with higher spatial resolution was chosen (US) to check homogeneity of lesion count and size between groups. US was able to show that the groups were homogeneous and that comparison between groups with PET at the end of the experiment was feasible. Although US is more sensitive in the detection of small lesions and offers good localization, it is not able to provide detailed information about tumor grade. Therefore we chose to use PET as a correlate for tumor aggression.

We showed that sorafenib could be responsible for reduced number of nodules and aggressiveness of HCC (more Grade I/II lesions than III/IV), as well as reduced tumor [¹⁸F]FDG uptake. [¹⁸F]FDG PET could be used

as a diagnostic tool for *in vivo* assessment of the degree of histological differentiation of HCC, since higher values of tracer uptake were correlated with more poorly differentiated HCC. Our methods and animal model, NAFLD, which exhibited progression to advanced HCC, will be useful for further studies of hepatic carcinogenesis.

DECLARATIONS

Acknowledgments

We would like to thank Mariana Maciel Torres and Edson Pereira da Costa for assistance with handling animals during this research. We want to thank Bayer Healthcare Pharmaceuticals for the donation of sorafenib.

Authors' contributions

Concept and design: Oliveira CP, Stefano JT, Carrilho FJ

Data acquisition: Costa FGB, Levy CS

Ultrasound work: Chammas MC

Pathology work: Pereira IVA, Cogliati B

Nuclear medicine work: Carneiro CG, Faria DP

Data analysis: Costa FGB, Stefano JT, Oliveira CP, Faria DP

Statistical analysis, literature search and manuscript preparation: Costa FGB

Manuscript editing: Costa FGB, Levy CS, Stefano JT, Oliveira CP, Faria DP

Manuscript review: Costa FGB, Stefano JT, Oliveira CP, Faria DP

Availability of data and materials

The data and materials could be obtained from the corresponding author.

Financial support and sponsorship

This work was supported by bursaries of Coordenação de Aperfeiçoamento de Pessoal de Nível Superior (CAPES) to Fernando Gomes de Barros Costa.

Conflicts of interest

All authors declare that there are no conflicts of interest.

Ethical approval and consent to participate

This study was approved by the ethical committee for animal use of the University of Sao Paulo Medical School (protocol 108/14).

Consent for publication

Not applicable.

Copyright

© The Author(s) 2018.

REFERENCES

1. European Association for the Study of the Liver (EASL); European Association for the Study of Diabetes (EASD); European Association for the Study of Obesity (EASO). EASL-EASD-EASO Clinical Practice Guidelines for the management of non-alcoholic fatty liver disease. *J Hepatol* 2016;64:1388-402.
2. Zoller H, Tilg H. Non-alcoholic fatty liver disease and hepatocellular carcinoma. *Metabolism* 2016;65:1151-60.
3. Machado MV, Diehl AM. Pathogenesis of nonalcoholic steatohepatitis. *Gastroenterology* 2016;150:1769-77.
4. Lozano R, Naghavi M, Foreman K, Lim S, Shibuya K, Aboyans V, Abraham J, Adair T, Aggarwal R, Ahn SY, Alvarado M, Anderson HR, Anderson LM, Andrews KG, Atkinson C, Baddour LM, Barker-Collo S, Bartels DH, Bell ML, Benjamin EJ, Bennett D, Bhalla K, Bikbov

- B, Bin Abdulhak A, Birbeck G, Blyth F, Bolliger I, Boufous S, Bucello C, Burch M, Burney P, Carapetis J, Chen H, Chou D, Chugh SS, Coffeng LE, Colan SD, Colquhoun S, Colson KE, Condon J, Connor MD, Cooper LT, Corriere M, Cortinovis M, de Vaccaro KC, Couser W, Cowie BC, Criqui MH, Cross M, Dabhadkar KC, Dahodwala N, De Leo D, Degenhardt L, Delossantos A, Denenberg J, Des Jarlais DC, Dharmaratne SD, Dorsey ER, Driscoll T, Duber H, Ebel B, Erwin PJ, Espindola P, Ezzati M, Feigin V, Flaxman AD, Forouzanfar MH, Fowkes FG, Franklin R, Fransen M, Freeman MK, Gabriel SE, Gakidou E, Gaspari F, Gillum RF, Gonzalez-Medina D, Halasa YA, Haring D, Harrison JE, Havmoeller R, Hay RJ, Hoen B, Hotez PJ, Hoy D, Jacobsen KH, James SL, Jasrasaria R, Jayaraman S, Johns N, Karthikeyan G, Kassebaum N, Keren A, Khoo JP, Knowlton LM, Kobusingye O, Koranteng A, Krishnamurthi R, Lipnick M, Lipshultz SE, Ohno SL, Mabweijano J, MacIntyre MF, Mallinger L, March L, Marks GB, Marks R, Matsumori A, Matzopoulos R, Mayosi BM, McAnulty JH, McDermott MM, McGrath J, Mensah GA, Merriman TR, Michaud C, Miller M, Miller TR, Mock C, Mocumbi AO, Mokdad AA, Moran A, Mulholland K, Nair MN, Naldi L, Narayan KM, Nasseri K, Norman P, O'Donnell M, Omer SB, Ortblad K, Osborne R, Ozgediz D, Pahari B, Pandian JD, Rivero AP, Padilla RP, Perez-Ruiz F, Perico N, Phillips D, Pierce K, Pope CA 3rd, Porrini E, Pourmalek F, Raju M, Ranganathan D, Rehm JT, Rein DB, Remuzzi G, Rivara FP, Roberts T, De León FR, Rosenfeld LC, Rushton L, Sacco RL, Salomon JA, Sampson U, Sanman E, Schwebel DC, Segui-Gomez M, Shepard DS, Singh D, Singleton J, Sliwa K, Smith E, Steer A, Taylor JA, Thomas B, Tleyjeh IM, Towbin JA, Truelsen T, Undurraga EA, Venketasubramanian N, Vijayakumar L, Vos T, Wagner GR, Wang M, Wang W, Watt K, Weinstock MA, Weintraub R, Wilkinson JD, Woolf AD, Wulf S, Yeh PH, Yip P, Zabetian A, Zheng ZJ, Lopez AD, Murray CJ, AlMazroa MA, Memish ZA. Global and regional mortality from 235 causes of death for 20 age groups in 1990 and 2010: a systematic analysis for the Global Burden of Disease Study 2010. *Lancet* 2012;380:2095-128.
5. Llovet J, Villanueva A, Lachenmayer A, Finn R. Advances in targeted therapies for hepatocellular carcinoma in the genomic era. *Nat Rev Clin Oncol* 2015;12:408-24.
 6. Rtveldadze K, Marsh T, Webber L, Kilpi F, Levy D, Conde W, McPherson K, Brown M. Health and economic burden of obesity in Brazil. *PLoS One* 2013;8:e68785.
 7. Wu J. Utilization of animal models to investigate non-alcoholic steatohepatitis-associated hepatocellular carcinoma. *Oncotarget* 2016;7:42762-76.
 8. Asgharpour A, Cazanave SC, Pacana T, Seneshaw M, Vincent R, Banini BA, Kumar DP, Daita K, Min HK, Mirshahi F, Bedossa P, Sun X, Hoshida Y, Koduru SV, Contaifer D Jr, Warncke UO, Wijesinghe DS, Sanyal AJ. A diet-induced animal model of non-alcoholic fatty liver disease and hepatocellular cancer. *J Hepatol* 2016;65:579-88.
 9. Tsatsoulis A, Mantzaris MD, Bellou S, Andrikoula M. Insulin resistance: an adaptive mechanism becomes maladaptive in the current environment - an evolutionary perspective. *Metabolism* 2013;62:622-33.
 10. Sanches SC, Ramalho LN, Augusto MJ, da Silva DM, Ramalho FS. Non-alcoholic steatohepatitis: a search for factual animal models. *Biomed Res Int* 2015;2015:574832.
 11. de Lima VM, Oliveira CP, Alves VA, Chammas MC, Oliveira EP, Stefano JT, de Mello ES, Cerri GG, Carrilho FJ, Caldwell SH. A rodent model of NASH with cirrhosis, oval cell proliferation, and hepatocellular carcinoma. *J Hepatol* 2008;49:1055-61.
 12. Groß C, Steiger K, Sayyed S, Heid I, Feuchtinger A, Walch A, Heß J, Unger K, Zitzelsberger H, Settles M, Schlitter AM, Dworniczak J, Altomonte J, Ebert O, Schwaiger M, Rummeny E, Steingötter A, Esposito I, Braren R. Model matters: differences in orthotopic rat hepatocellular carcinoma physiology determine therapy response to sorafenib. *Clin Cancer Res* 2015;21:4440-50.
 13. Park JH, Kang JH, Lee YJ, Kim KI, Lee TS, Kim KM, Park JA, Ko YO, Yu DY, Nahm SS, Jeon TJ, Park YS, Lim SM. Evaluation of diethylnitrosamine- or hepatitis B virus X gene-induced hepatocellular carcinoma with 18F-FDG PET/CT: a preclinical study. *Oncol Rep* 2015;33:347-53.
 14. Carvalho CF, Chammas MC, Souza de Oliveira CP, Cogliati B, Carrilho FJ, Cerri GG. Elastography and contrast-enhanced ultrasonography in the early detection of hepatocellular carcinoma in an experimental model of non-alcoholic steatohepatitis. *J Clin Exp Hepatol* 2013;3:96-101.
 15. Park SI, Lee JH, Ham HJ, Jung YJ, Park MS, Lee J, Maeng LS, Chung YA, Jang KS. Evaluation of 2-[18F]-fluoro-2-deoxy-D-glucose positron emission tomography/computed tomography in rat models with hepatocellular carcinoma with liver cirrhosis. *Biomed Mater Eng* 2015;26 Suppl 1:S1669-76.
 16. Cho E, Jun CH, Kim BS, Son DJ, Choi WS, Choi SK. 18F-FDG PET CT as a prognostic factor in hepatocellular carcinoma. *Turk J Gastroenterol* 2015;26:344-50.
 17. Kim YI, Paeng JC, Cheon GJ, Suh KS, Lee DS, Chung JK, Kang KW. Prediction of post-transplantation recurrence of hepatocellular carcinoma using metabolic and volumetric indices of 18F-FDG PET/CT. *J Nucl Med* 2016;57:1045-51.
 18. Sun DW, An L, Wei F, Mu L, Shi XJ, Wang CL, Zhao ZW, Li TF, Lv GY. Prognostic significance of parameters from pretreatment (18)F-FDG PET in hepatocellular carcinoma: a meta-analysis. *Abdom Radiol (NY)* 2016;41:33-41.
 19. Lee SD, Lee B, Kim SH, Joo J, Kim SK, Kim YK, Park SJ. Proposal of new expanded selection criteria using total tumor size and (18)F-fluorodeoxyglucose - positron emission tomography/computed tomography for living donor liver transplantation in patients with hepatocellular carcinoma: The National Cancer Center: Korea criteria. *World J Transplant* 2016;6:411-22.
 20. Detry O, Govaerts L, Deroover A, Vandermeulen M, Meurisse N, Malenga S, Bletard N, Mbendi C, Lamproye A, Honoré P, Meunier P, Delwaide J, Hustinx R. Prognostic value of (18)F-FDG PET/CT in liver transplantation for hepatocarcinoma. *World J Gastroenterol* 2015;21:3049-54.
 21. Kornberg A, Küpper B, Tannapfel A, Büchler P, Krause B, Witt U, Gottschild D, Friess H. Patients with non-[18 F]fludeoxyglucose-avid advanced hepatocellular carcinoma on clinical staging may achieve long-term recurrence-free survival after liver transplantation. *Liver Transpl* 2012;18:53-61.
 22. Brito AF, Abrantes AM, Ribeiro M, Oliveira R, Casalta-Lopes J, Gonçalves AC, Sarmento-Ribeiro AB, Tralhão JG, Botelho MF.

- Fluorine-18 fluorodeoxyglucose uptake in hepatocellular carcinoma: correlation with glucose transporters and p53 expression. *J Clin Exp Hepatol* 2015;5:183-9.
23. Lee SD, Kim SH, Kim YK, Kim C, Kim SK, Han SS, Park SJ. (18)F-FDG-PET/CT predicts early tumor recurrence in living donor liver transplantation for hepatocellular carcinoma. *Transpl Int* 2013;26:50-60.
 24. European Association For The Study Of The Liver; European Organisation For Research And Treatment Of Cancer. EASL-EORTC clinical practice guidelines: management of hepatocellular carcinoma. *J Hepatol* 2012;56:908-43.
 25. Bruix J, Han KH, Gores G, Llovet JM, Mazzaferro V. Liver cancer: approaching personalized care. *J Hepatol* 2015;62:S144-56.
 26. Yoshiji H, Noguchi R, Namisaki T, Moriya K, Kitade M, Aihara Y, Douhara A, Kawaratani H, Nishimura N, Fukui H. Combination of sorafenib and angiotensin-II receptor blocker attenuates preneoplastic lesion development in a non-diabetic rat model of steatohepatitis. *J Gastroenterol* 2014;49:1421-9.
 27. Edginton AN, Zimmerman EI, Vasilyeva A, Baker SD, Panetta JC. Sorafenib metabolism, transport, and enterohepatic recycling: physiologically based modeling and simulation in mice. *Cancer Chemother Pharmacol* 2016;77:1039-52.
 28. Wilhelm SM, Carter C, Tang L, Wilkie D, McNabola A, Rong H, Chen C, Zhang X, Vincent P, McHugh M, Cao Y, Shujath J, Gawlak S, Eveleigh D, Rowley B, Liu L, Adnane L, Lynch M, Auclair D, Taylor I, Gedrich R, Voznesensky A, Riedl B, Post LE, Bollag G, Trail PA. BAY 43-9006 exhibits broad spectrum oral antitumor activity and targets the RAF/MEK/ERK pathway and receptor tyrosine kinases involved in tumor progression and angiogenesis. *Cancer Res* 2004;64:7099-109.
 29. Stefano JT, Pereira IV, Torres MM, Bida PM, Coelho AM, Xerfan MP, Cogliati B, Barbeiro DF, Mazo DF, Kubrusly MS, D'Albuquerque LA, Souza HP, Carrilho FJ, Oliveira CP. Sorafenib prevents liver fibrosis in a non-alcoholic steatohepatitis (NASH) rodent model. *Br J Med Biol Res* 2015;48:408-14.
 30. Yang YY, Liu RS, Lee PC, Yeh YC, Huang YT, Lee WP, Lee KC, Hsieh YC, Lee FY, Tan TW, Lin HC. Anti-VEGFR agents ameliorate hepatic venous dysregulation/microcirculatory dysfunction, splanchnic venous pooling and ascites of NASH-cirrhotic rat. *Liver Int* 2014;34:521-34.
 31. Carvalho CF, Chammas MC, Souza de Oliveira CPM, Cogliati B, Carrilho FJ, Cerri GG. Elastography and contrast-enhanced ultrasonography in the early detection of hepatocellular carcinoma in an experimental model of nonalcoholic steatohepatitis. *J Clin Exp Hepatol* 2013;3:96-101.
 32. Rapisarda E, Bettinardi V, Thielemans K, Gilardi MC. Image-based point spread function implementation in a fully 3D OSEM reconstruction algorithm for PET. *Phys Med Biol* 2010;55:4131-51.
 33. Kleiner DE, Brunt EM, Van Natta M, Behling C, Contos MJ, Cummings OW, Ferrell LD, Liu YC, Torbenson MS, Unalp-Arida A, Yeh M, McCullough AJ, Sanyal AJ; Nonalcoholic Steatohepatitis Clinical Research Network. Design and validation of a histological scoring system for nonalcoholic fatty liver disease. *Hepatology* 2005;41:1313-21.
 34. Thoolen B, Maronpot RR, Harada T, Nyska A, Rousseaux C, Nolte T, Malarkey DE, Kaufmann W, Küttler K, Deschl U, Nakae D, Gregson R, Vinlove MP, Brix AE, Singh B, Belpoggi F, Ward JM. Proliferative and nonproliferative lesions of the rat and mouse hepatobiliary system. *Toxicol Pathol* 2010;38:S5-81.
 35. Schlageter M, Terracciano LM, D'Angelo S, Sorrentino P. Histopathology of hepatocellular carcinoma. *World J Gastroenterol* 2014;20:15955-64.
 36. Mattina J, MacKinnon N, Henderson VC, Fergusson D, Kimmelman J. Design and reporting of targeted anticancer preclinical studies: a meta-analysis of animal studies investigating sorafenib antitumor efficacy. *Cancer Res* 2016;76:4627-36.
 37. Villanueva A, Llovet JM. Targeted therapies for hepatocellular carcinoma. *Gastroenterology* 2011;140:1410-26.
 38. Abou-Alfa GK, Schwartz L, Ricci S, Amadori D, Santoro A, Figer A, De Greve J, Douillard JY, Lathia C, Schwartz B, Taylor I, Moscovici M, Saltz LB. Phase II study of sorafenib in patients with advanced hepatocellular carcinoma. *J Clin Oncol* 2006;24:4293-300.
 39. Cho Y, Lee DH, Lee YB, Lee M, Yoo JJ, Choi WM, Cho YY, Paeng JC, Kang KW, Chung JK, Yu SJ, Lee JH, Yoon JH, Lee HS, Kim YJ. Does 18F-FDG positron emission tomography-computed tomography have a role in initial staging of hepatocellular carcinoma? *PLoS One* 2014;9:e105679.